Extended Abstracts of the 2004 International Conference on Solid State Devices and Materials, Tokyo, 2004, pp. 464-465

P3-10

Work function control of Al-Ni alloy for metal gate application

T. Matsukawa, C. Yasumuro, H. Yamauchi, S. Kanemaru, M. Masahara, K. Endo, E. Suzuki and J. Itoh
Nanoelectronics Research Institute, AIST, 1-1-1 Umezono, Tsukuba, Ibaraki 305-8568, Japan
Phone: +81-29-861-5358, Fax: +81-29-861-5507, E-mail: t-matsu@aist.go.jp

1. Introduction

Introduction of metal gates is an effective solution for gate depletion and boron penetration problems of poly-silicon gates in conventional MOSFETs. In case of metal-gate transistors, especially in FD-SOI and double gate structures, the threshold voltage (V_{th}) is dominantly determined by the work function of the metal (ϕ_m) [1]. Thus, ϕ_m adjustment is essential to obtain the optimum V_{th} and is possible by a binary alloy of metals with different ϕ_m [2,3]. In this study, we investigate applicability of the alloy of Al with low ϕ_m (4.28 eV) and Ni with high ϕ_m (5.15 eV) [4]. The Al-Ni alloy has higher thermal stability than pure Al. We found that the $Al_{50}Ni_{50}$ alloy exhibits ϕ_m approximately at the middle the ϕ_m's of Al and Ni. Spatial variation of ϕ_m evaluated by a microscopic way depends on the process of the alloy film formation. Thermal stability of the alloy film against the S/D extension activation is also evaluated.

2. Experimental

The Al-Ni alloy MOS capacitors were fabricated by 2 different processes, i.e., an "interdiffusion" and a "direct sputtering" process (Fig. 1). In the interdiffusion process, the layered structure (Ni/Al) was formed by evaporating Al (60 nm) and Ni (39 nm) subsequently. The thickness was determined to obtain the atomic composition of Al and Ni of 50:50. The layered structure was then annealed (500ºC, 1 h) and the alloy was fabricated by interdiffusion of Al and Ni. Cross section of MOS structures was observed by STEM Z-contrast. In the STEM image of Ni/Al before the interdiffusion (Fig. 2(a)), Ni with a bright and Al with a dark contrast are recognized clearly. It is remarked in Fig. 2(b) that, after the interdiffusion, the layered contrast disappears and the interdiffusion of Al and Ni almost completes while the different contrast among grains is noticeable. In the direct sputtering process, on the other hand, the Al-Ni alloy (100 nm) was directly deposited by sputtering an $Al_{50}Ni_{50}$ target. The cross section of the sputtered Al-Ni film shows a smooth surface and uniform contrast (Fig. 2(c)). A diameter of the Al-Ni pad was 500 μm. CV curves were measured after forming-gas annealing.

3. Results and Discussion

CV curves of the Al-Ni alloy MOS capacitor with a 5nm-thick oxide were compared with those of pure Al and Ni ones (Fig. 3). The curve of the Ni/Al interdiffused alloy sample exhibits positive shift and significant decrease in the slope in comparison with that of the pure Al sample. For the sputtered Al-Ni sample, only the positive shift from that of the pure Al sample is observed. In order to estimate ϕ_m, a flat band voltage (V_{fb}) and an equivalent oxide thickness (EOT) were extracted from the CV data. V_{fb} vs. EOT (Fig. 4) for all metal species exhibits linear relation, which enables us to estimate ϕ_m from the y-intercept. As shown in Table I, ϕ_m's estimated from the CV data for Al (4.353 eV) and Ni (5.017 eV) are almost coincided with the reported values [4]. Work function ϕ_m's for both the interdiffused (4.621 eV) and sputtered (4.565 eV) Al-Ni alloys fall on approximately at the middle of Al and Ni. Thus, it is concluded that both the interdiffusion and sputtering processes can control ϕ_m of the Al-Ni alloys.

Scanning Maxwell-stress microscopy (SMM) [5], which is capable to measure the contact potential difference (CPD) between the probe and sample, was used to estimate the spatial variation of ϕ_m. Average values of CPD in 2 x 2 μm^2 scan areas on Al, Ni, and Al-Ni alloys were converted to ϕ_m's (Table I). The estimated ϕ_m's are almost coincided with those estimated from the CVs and those reported in the reference [4]. Thus, ϕ_m evaluated by SMM can be used for prediction of the electrical characteristics of metal gates. The CPD distribution obtained by SMM (Fig. 5) represents the spatial variation of ϕ_m, where a higher CPD value corresponds to lower ϕ_m. While the Ni film (Fig. 5(a)) exhibits uniform CPD, the Al/Ni interdiffused alloy (Fig. 5(b)) shows remarkably nonuniform CPD. It should be noted therefore that the interdiffusion process causes significant nonuniformity of ϕ_m in the film. In this case, the CV curve reflects both the local capacitance components at low and high ϕ_m portions, resulting in decrease in the slope of the CV curve (Fig. 6). Thus, the ϕ_m nonuniformity is the reason for the degraded CV slope for the Al-Ni interdiffused alloy shown in Fig. 3. In case of the sputtered Al-Ni film, on the other hand, the CPD became uniform (Fig. 5(c)), i.e., the ϕ_m distribution is uniform. Therefore, the direct sputtering process of the Al-Ni alloy is preferable to suppress the ϕ_m nonuniformity.

Stability against the dopant activation annealing is important issue for metal gates. Recently, the successful dopant activation using solid phase epitaxy at 650ºC for 1 min was reported [6]. We examined the stability of the Al-Ni sputtered alloy against the thermal budget of 700ºC, 1 min. The CV curve after the thermal budget (Fig. 7) exhibits no significant degradation although it shows the slightly positive shift. V_{fb} vs. EOT (Fig. 8) after the thermal budget shows the linear relationship; namely, the thermal budget causes no damage in the oxide. Although the thermal budget results in increased in ϕ_m (4.722 eV), the ϕ_m is still in the middle of Al and Ni. This result indicates the possibility of the gate-first process using the Al-Ni alloy.

4. Conclusions

The work function control of metal gates was carried out using Al-Ni alloys with the interdiffusion and the direct sputtering processes. The CV curves exhibited same ϕ_m for both the processes. Since the SMM measurement revealed that the interdiffused Al-Ni alloy had significant ϕ_m nonuniformity which could cause V_{th} fluctuation, direct sputtering of Al-Ni alloy is the preferable process.

References

[1] L. Chang *et al.*, *IEDM* (2000) 719. [2] H. Zhong *et al.*, *IEDM* (2001) 467. [3] I. Polishchuk *et al.*, *IEEE EDL* **23** (2002) 200. [4] H. Michelson, *IBM. J. Res. Develop.* **22** (1978) 72. [5] T. Matsukawa *et al.*, *JVST.* **B19** (2001) 1911. [6] R. Lindsay *et al.*, *Ext. Abst. IWJT* (2004) 70.

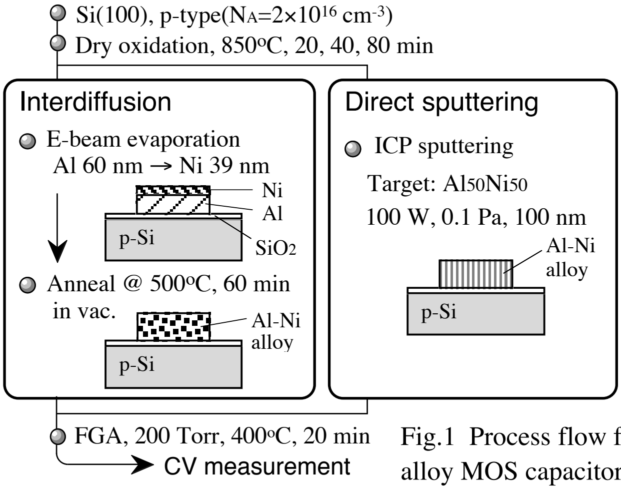

Fig.1 Process flow for alloy MOS capacitors.

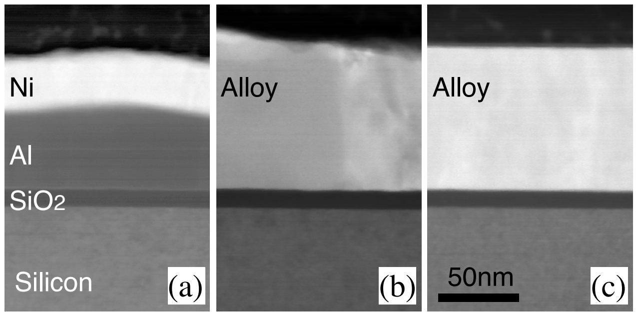

Fig.2 Cross section of MOS structures by STEM Z-contrast. (a) Ni/Al before and (b) after interdiffusion, and (c) direct-sputtered Al-Ni alloy.

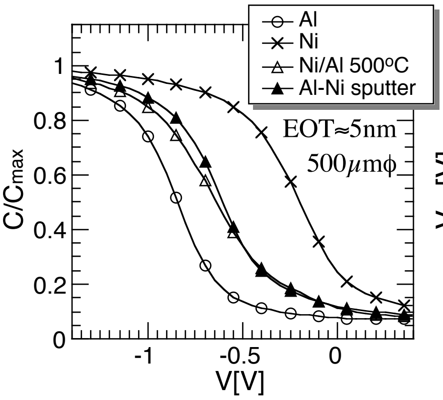

Fig.3 Comparison of CVs among Al-Ni alloys, Al and Ni.

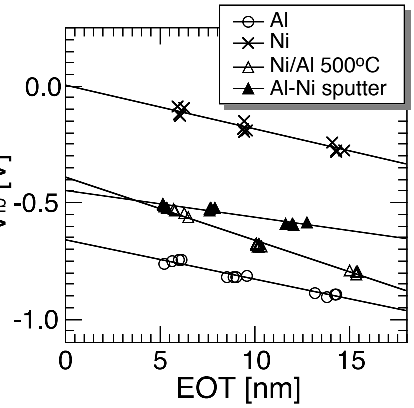

Fig.4 V_{fb} vs. EOT for work function estimation.

Table I. Summary of work function values

Metal species	Work function ϕ_m [eV]		
	Reported [4]	CV	SMM
Al	4.28	4.353	4.208
Ni	5.15	5.017	5.063
Ni/Al 500°C	-	4.621	4.601*
Al-Ni sputter	-	4.565	4.676

* In order to reproduce Ni/Al interdiffused MOS where Al is initially in contact with SiO_2, Al/Ni was interdiffused and measured by SMM.

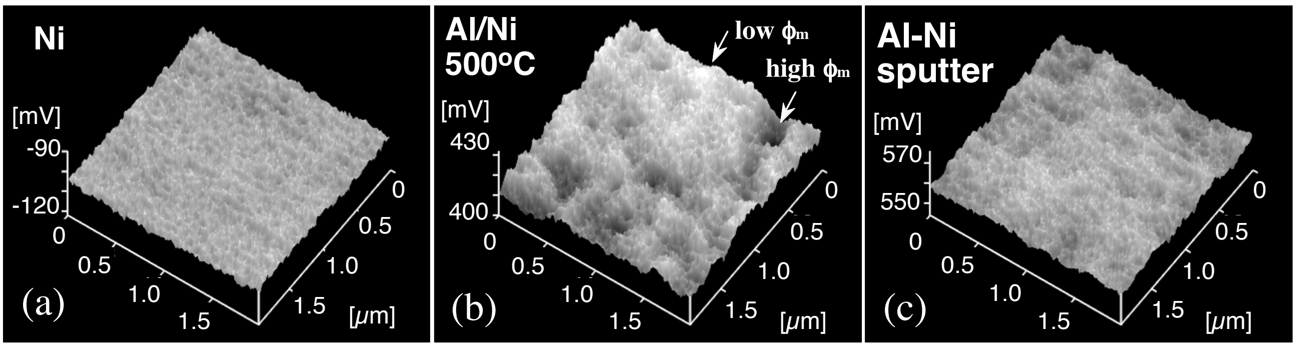

Fig.5 CPD distribution obtained by SMM. (a) Ni, (b) Al/Ni interdiffused, and (c) Al-Ni sputtered films.

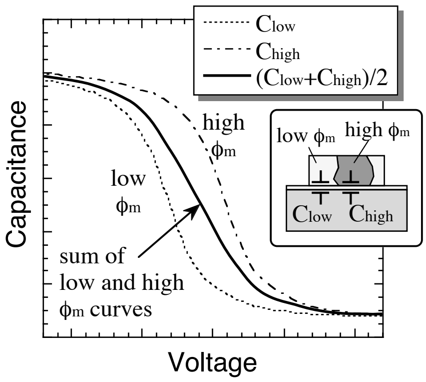

Fig.6 Simple model of CV characteristics with spatial variation of work function.

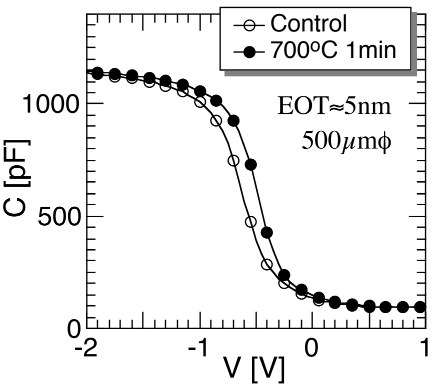

Fig.7 Influence of thermal budget on CVs for Al-Ni sputtered film.

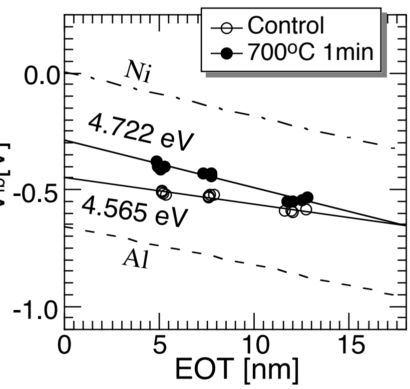

Fig.8 V_{fb} vs. EOT after thermal budget.